Available online at www.sciencedirect.com
SCIENCE DIRECT®
Surface Science 574 (2005) 166–174
SURFACE SCIENCE
www.elsevier.com/locate/susc

The structure of formate species on Pd(1 1 1) calculated by density functional theory and determined using low energy electron diffraction

T. Zheng [a], D. Stacchiola [a], D.K. Saldin [b], J. James [c], D.S. Sholl [c], W.T. Tysoe [a,*]

[a] *Department of Chemistry and Biochemistry, Laboratory for Surface Studies, University of Wisconsin-Milwaukee, 3210 N. Cramer Street, Milwaukee, WI 53211, USA*
[b] *Department of Physics, Laboratory for Surface Studies, University of Wisconsin-Milwaukee, Milwaukee, WI 53211, USA*
[c] *Department of Chemical Engineering, Carnegie Mellon University, Pittsburgh, PA 15213, USA*

Received 1 September 2004; accepted for publication 19 October 2004
Available online 13 December 2004

Abstract

The structure of formate species adsorbed on Pd(1 1 1) has been determined using low-energy electron diffraction (LEED). The presence of formate species on the Pd(1 1 1) surface was established using reflection-absorption infrared spectroscopy (RAIRS). The oxygen atoms of the formate species were found to be adsorbed over surface palladium atoms with the OCO plane perpendicular to the surface. The CO bond length was found to be 1.26 ± 0.05 Å, the palladium–oxygen distance was 2.16 ± 0.06 Å, and the OCO angle $130 \pm 5°$. The experimentally determined values were in excellent agreement with those calculated using density functional theory (DFT).

Keywords: Palladium; Formic acid; Infrared spectroscopy; Low energy electron diffraction (LEED); Surface structure, morphology, roughness, and topography; Density functional theory

1. Introduction

The participation of carboxylate intermediates has been invoked in a number of catalytic reactions including the water-gas shift reaction [1], methanol synthesis and decomposition [2–6], and the methanation of CO and CO_2 [7–12]. As an example, the reaction pathway for the synthesis of oxygenates from CO and hydrogen invokes the formation of a stable carboxylate that hydrogenates to yield alcohols over supported group-VIII transition-metal catalysts [13–15]. Carboxylates

* Corresponding author. Tel.: +1 414 229 5222; fax: +1 414 229 5036.
E-mail address: wtt@uwm.edu (W.T. Tysoe).

0039-6028/$ - see front matter © 2004 Elsevier B.V. All rights reserved.
doi:10.1016/j.susc.2004.10.027

(in this case acetates) are also proposed to be intermediates in the palladium-catalyzed synthesis of vinyl acetate monomers from ethylene, acetic acid and oxygen [16,17]. The decomposition of formates ($HCOO^-$) [18–32] and acetates (CH_3COO^-) [33–37] has been studied on a number of single crystal surfaces. In spite of the importance of these species as catalytic intermediates, there have been remarkably few structural studies of carboxylates on single-crystal, transition-metal surfaces. This is partly due to the fact that they do not tend to form ordered structures and are therefore not amenable to analysis by standard low-energy electron diffraction (LEED) methods. Photoelectron diffraction has been used to measure the structure of formate [38,39] and acetate [40] species on copper where the oxygen atoms are found to be located above copper atoms with the OCO plane oriented perpendicular to the surface with an OCO bond angle of ~124°.

We have recently shown that it is possible to use conventional LEED methods to measure the structures of disordered overlayers by interrogating the way in which the intensities of the substrate (1×1) Bragg diffraction spots are modified by the presence of an overlayer [41–43]. This strategy is applied in the following to measuring the structure of formate species on Pd(1 1 1) where no ordered LEED patterns are observed. An additional advantage of this method is that the adsorbate coverage appears as a variable in the analysis and thus provides an additional method of determining surface coverages.

Finally, we have recently shown that amino acids can act as chiral templates for the adsorption of propylene oxide on Pd(1 1 1) [44]. That is, precovering a Pd(1 1 1) surface with either an *R*- or *S*-amino acid preferentially adsorbs propylene oxide of the same chirality. A detailed knowledge of the structure of the amino acids on surfaces is central to understanding this behavior. Since the amino acids are more complex than the carboxylic acids, it is not feasible to vary all geometrical parameters to find the best fit to the LEED intensity versus beam energy (*I*/*E*) curves. In such cases, it would be extremely beneficial to have structures calculated by density functional theory (DFT) as inputs into the LEED calculations. We have therefore compared the results of structural measurements by LEED with the results of DFT on Pd(1 1 1). One goal of this work, therefore, is to test how well DFT can predict the measured structure for carboxylates on Pd(1 1 1).

2. Methods

2.1. Experimental methods

LEED measurements were carried out in a doubly μ-metal shielded ultrahigh vacuum chamber operating at a base pressure of 5×10^{-11} Torr, and containing a Pd(1 1 1) single crystal, which could be cooled to 80 K and resistively heated to 1200 K. The sample was cleaned using standard procedures. LEED patterns of the clean surface were photographed as a function of incident energy using a Nikon Coolpix digital camera (5.0 MBytes resolution) and the images stored on an IBM Smartcard memory (1 GByte). The images were then downloaded to a personal computer for subsequent analysis using NIHIMage [45]. Images were initially collected for the clean surface every 5 eV between 80 and 325 eV, a procedure that took approximately 15 min. The sample was heated briefly to 740 K to remove any background contaminants that may have adsorbed during this process. The surface was then exposed to formic acid and the LEED *I*/*E* curve of the formate-covered surface was collected. The reflection-absorption infrared spectra (RAIRS) were collected in ultrahigh vacuum as described in detail elsewhere [46]. All spectra were collected at $4\,cm^{-1}$ resolution for 1000 scans.

The formate species were formed by dosing 5 L of formic acid (Aldrich, 99%) at 170 K and then heating briefly to 200 K resulting in the formation of a saturated overlayer. The sample was then allowed to cool to 80 K and the *I*/*E* curve collected.

2.2. Theoretical methods

The *I*/*E* data from the clean surface were first analyzed by comparison with standard LEED calculations [42] to determine the incidence angle of the electrons relative to the surface. The *I*/*E* curves

from the formate-covered sample were then simulated for this angle of incidence by assuming an ordered overlayer of the smallest possible (1×1) periodicity with fractional occupancy of the same magnitude as the coverage Θ. The notion that a calculation involving only integer-order beams may be sufficiently accurate for practical calculations of the integer-order Bragg spots for large unit-cell overlayers may be regarded as a special case of the beam set neglect method [47,48]. The extra simplification introduced in the present paper is that the quasidynamical [49] treatment of the adlayer allows it to be treated as literally a (1×1) overlayer with an adsorbate scattering factor reduced by a factor of Θ, so that the coverage appears as a variable in the LEED structure determination. The precision of the bond lengths was determined in standard way from the change the in Pendry R-factor [50] as a function of change in geometrical parameters.

Plane wave density functional theory calculations were performed using the Vienna ab initio simulation package (VASP) [51]. VASP has been shown to give results that are in agreement with other DFT packages [52,53]. The results reported here are from calculations using the spin polarized generalized gradient approximation (GGA) with a $3 \times 3 \times 1$ k-point mesh. To examine the structure of isolated formate molecules on Pd(1 1 1), all calculations placed a single adsorbed molecule in a (3×3) surface unit cell. The Pd (1 1 1) surface was represented by a slab four layers thick and a vacuum spacing of 14 Å. The DFT-optimized lattice constant for Pd was used to define the surface. This lattice constant, 3.96 Å, is in good agreement with the experimental value of 3.89 Å [54]. The top two layers of the slab were allowed to relax with the adsorbed molecule, since the adsorbate is expected to exhibit some effect on the substrate. All calculations involved convergence of relaxed atomic forces to within 0.03 eV/Å.

3. Results

The RAIRS spectrum of formic acid adsorbed on Pd(1 1 1) at 150 K is displayed in Fig. 1 as a function of formic acid exposure, where the exposures (in Langmuirs, $1\,L = 1 \times 10^{-6}$ Torr) are marked adjacent to the corresponding spectrum. At low exposures, the spectrum consists of three relatively sharp features at 792, 1342 and 2904 cm^{-1}. These features persist as the exposure increases, and additional peaks are detected at 947, 1243, 1630 and 1704 cm^{-1} after an exposure of 0.6 L of formic acid. These features become more intense as the exposure increases further until the formic acid multilayer spectrum is evident after dosing 1 L. These features can be assigned straightforwardly by comparison with the spectra of formic acid on Pt(1 1 1) [20] and the assignments are summarized in Tables 1 and 2. This reveals that the features at 792, 1342 and 2904 cm^{-1} are due to formate species, while those at 947, 1243, 1630 and 1704 cm^{-1} are due to adsorbed formic acid. Evidently the spectra in Fig. 1 indicate that formate species initially form on the surface following

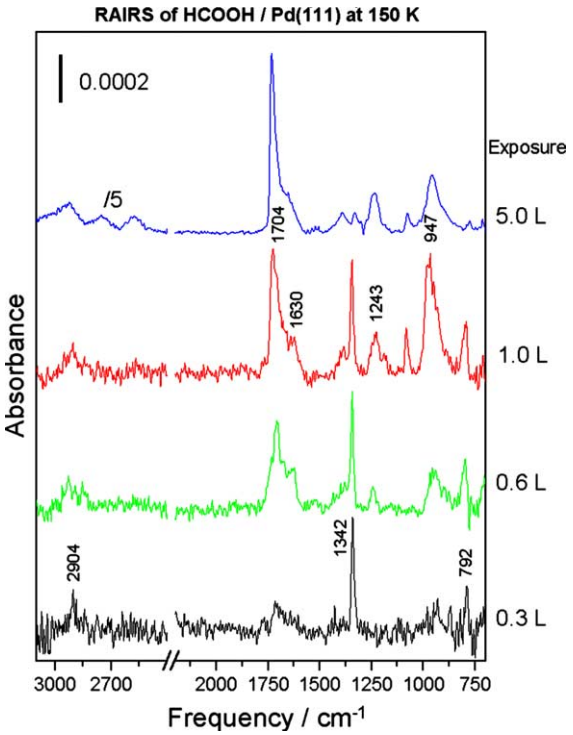

Fig. 1. RAIRS spectra of formic acid adsorbed on clean Pd(1 1 1) at 150 K as a function of formic acid exposure, where exposures are marked adjacent to the corresponding spectrum.

Table 1
Assignment of the vibrational modes of formate species on Pd(1 1 1)

Assignment	Frequency/cm^{-1}	
	Formate/Pt(1 1 1) [20]	Formate/Pd(1 1 1) (This work)
δ (OCO)	790	792
ν_s (OCO)	1340	1342
ν (CH)	2950	2904

Table 2
Assignment of the vibrational modes of formic acid on Pd(1 1 1)

Assignment	Frequency/cm^{-1}	
	Formic acid/Pt(1 1 1) [20]	Formic acid/Pd(1 1 1) (This work)
ν (C=O)	1720	1704
ν (C=O)	1640	1630
ν (CO)	1230	1243
π (OH)	980	947

small exposures at 150 K and molecular formic acid adsorbs thereafter.

Fig. 2 shows the changes in the spectra on heating to 175 and 200 K. The intensities of the features due to molecular formic acid decrease on heating to 175 K and are completely absent when the surface is heated to 200 K, where features due to only formate species are present. The formate species can also be formed directly by dosing the surface with formic acid at 200 K. Heating the surface to 220 K causes a strong diminution in the intensities of the formate modes, which disappear completely on heating to 230 K. These observations are in complete accord with the temperature-programmed desorption (TPD) spectra of formic acid on Pd(1 1 1) [55], except that CO desorption is found in TPD, while no CO is detected in the infrared spectra. It should be noted that DFT and Monte Carlo simulations of the TPD spectra of formic acid on Pd(1 1 1) found no CO formation pathways [56] indicating that the CO found in TPD was due to CO adsorption from the background.

Based on the infrared results, formate species were formed on Pd(1 1 1) by exposure to 5 L of formic acid at 170 K and heating briefly to 200 K. The

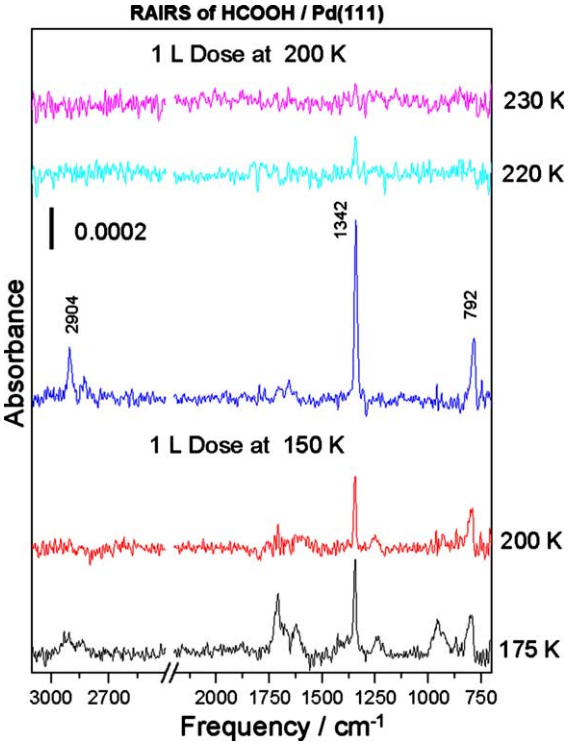

Fig. 2. RAIRS spectra of 1 L of formic acid adsorbed on Pd(1 1 1) at 150 K heated to 175 and 200 K, where the temperatures are marked adjacent to the corresponding spectra. Shown also are the spectra obtained following a 1 L formic acid exposure at 200 K and by subsequently heating to 220 and 230 K.

resulting experimentally observed I/E curves of the (1×1) diffraction spots are displayed in Fig. 3 (solid lines). The resulting calculated curves for the best structure (see below) are also plotted as dashed lines. Based on the observation that formate species form on copper with the OCO plane perpendicular to the surface with an OCO bond angle of ~124° [38–40], a global search was carried out to determine the adsorption site by initially fixing this geometry. This geometry is also consistent with the infrared spectrum (see below). In addition, based on the observation that acetate species have a saturation coverage of 0.25 on copper surfaces [38], the formate coverage was fixed at this value. The C–O bond length was initially fixed at 1.25 Å also based on the value measured on the copper surface [38–40]. The global search was

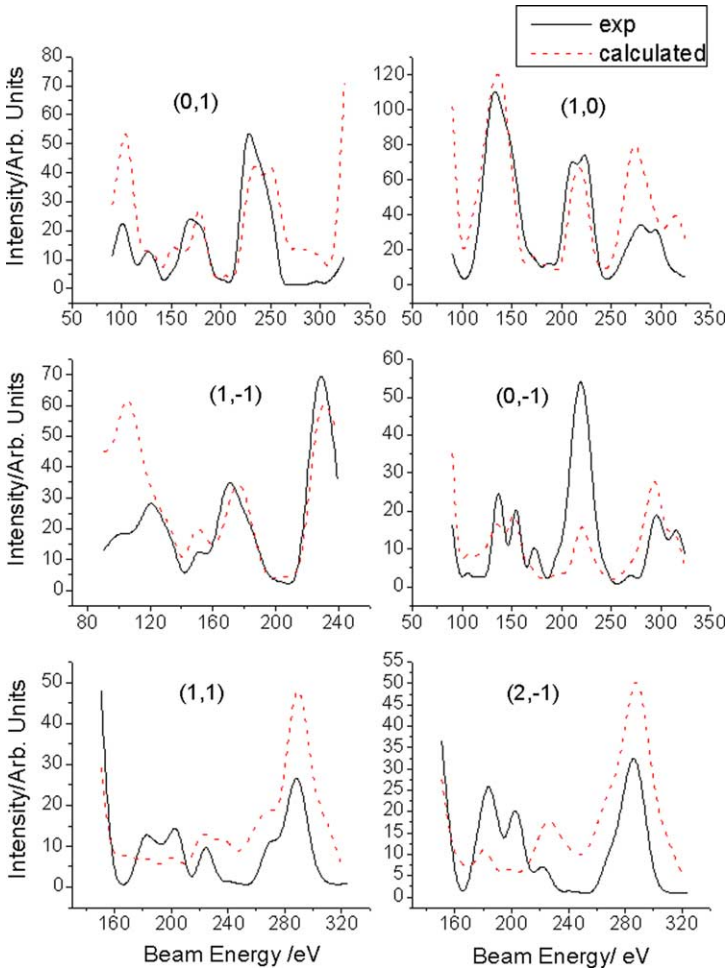

Fig. 3. Experimental *I*/*E* curves for a disordered overlayer of formate species on a Pd(1 1 1) surface (solid lines). Shown for comparison are the calculated curves for the best-fit structure (dashed lines).

carried out by allowing one of the oxygen atoms to adsorb at a total of 21 points in a reduced Wigner–Seitz cell on the (1 1 1) surface without allowing the substrate palladium atoms to relax. The *z*-distance of the oxygen atoms to the surface was then varied between 1.7 and 2.1 Å in steps of 0.1 Å and the formate species allowed to rotate azimuthally about a normal to the Pd(1 1 1) surface in steps of 30°. The resulting contour plot of Pendry *R*-factors [50], for the *z*-height and azimuthal angle that gave the lowest Pendry *R*-factor, is displayed in Fig. 4 for a *z*-height of 2.1 Å, as a function of position within the reduced Wigner-Seitz cell. The minimum value of the *R*-factor is 0.46, which allows sites for which the *R*-factor is greater than ~0.50 to be excluded [50] eliminating the possibility that the oxygen atom adsorbs directly above one of the high-symmetry (atop, bridge, and fcc and hcp hollow) sites. There are two shallow minima within the central region of the Wigner Seitz cell marked A and B. These structures were further refined using tensor LEED while allowing the palladium atom positions to relax [57]. It should be noted that this is similar to a linear least-squares fitting program so that the initial structure must be close to the "true" structure for the program

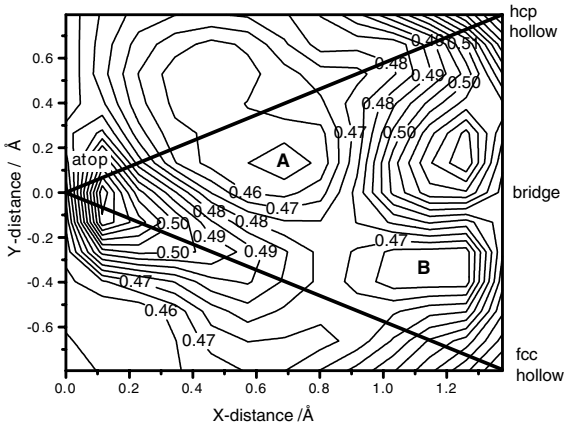

Fig. 4. Contour plot of the Pendry *R*-factor as a function of the position of an O atom of the formate species within the reduced Wigner–Seitz cell of Pd(1 1 1). The height of the O atom above the surface was optimized by allowing it to vary between 1.7 and 2.1 Å in steps of 0.1 Å, and the azimuthal angle of the molecular plane optimized by allowing it to vary in steps of 30.

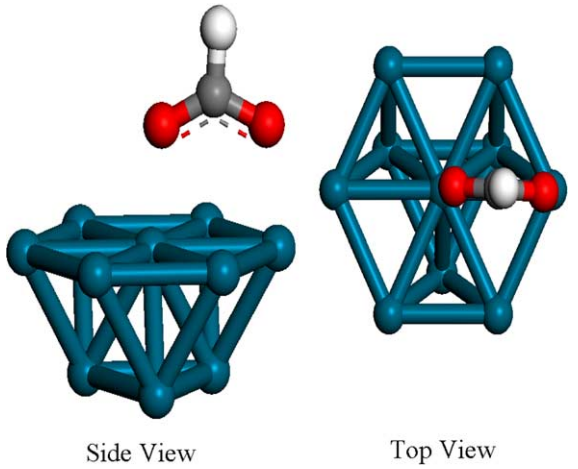

Fig. 5. Depiction of the structure of formate species adsorbed on Pd(1 1 1) from LEED.

Table 3
Theoretical and experimental geometrical parameters for formate species on Pd(1 1 1)

	Formate/Pd(1 1 1) from LEED	Formate/Pd(1 1 1) from DFT
d(O–Pd)/Å	2.16 ± 0.06	2.13
Angle of OCO plane to surface/°	90 ± 2	90
OCO angle/°	130 ± 5	129
d(C–O)/Å	1.26 ± 0.05	1.27
d(C–H)/Å	–	1.1

to converge properly. Initial structures around "B" did not converge. The azimuthal angle around point "A" corresponds to the OCO plane oriented along a line joining the atop and bridge sites so that structure with the carbon atom above the bridge site was used as an input into the tensor LEED program, which successfully converged. Finally, the tensor LEED calculation was performed for various formate coverages between 0.2 and 0.45 using the refined structure. This revealed that the formate coverage was ~0.23, in good agreement with that found on Cu(1 0 0) [38].

Only slight changes were noted from the structure found from the global search following the Tensor LEED calculation for a formate coverage of 0.23, leading to a final Pendry *R*-factor of ~0.33. The azimuthal OCO angle, the angle of the OCO plane to the surface, and the *z*-distance of the oxygen atoms from the surface all remained unchanged. The final experimental formate structure is depicted in Fig. 5 and the corresponding geometrical parameters summarized in Table 3. The errors in the experimental measurements were estimated in the standard way by calculating the variation in the Pendry *R*-factor for each parameter. Although no CO was found on the surface using infrared spectroscopy following formic acid adsorption on Pd(1 1 1) (Figs. 1 and 2), this was further checked by comparing the experimental LEED *I*/*E* data for a surface covered by both formate species and CO. The resulting plot of Pendry *R*-factor versus CO coverage is displayed in Fig. 6 and shown a minimum at $\Theta(\mathrm{CO}) = 0.01 \pm 0.04$ and is in accord with the RAIRS data showing that no CO is formed by formate decomposition.

4. Discussion

The vibrational frequencies of formate species formed on Pd(1 1 1) are in good agreement with those found on Pt(1 1 1) [20] (Table 1, Figs. 1 and 2). The symmetric OCO mode appears at 1342 cm^{-1} on Pd(1 1 1), while no corresponding

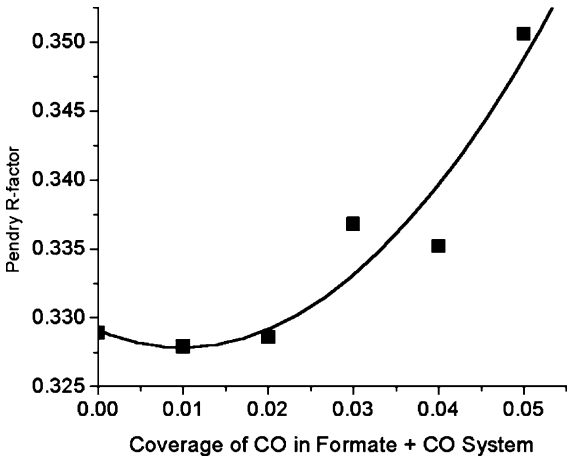

Fig. 6. Plot of Pendry *R*-factor versus coverage of CO co-adsorbed with formate species on Pd(1 1 1).

asymmetric mode is observed indicating that the OCO plane of the formate is oriented perpendicular to the surface. Some formate species form on the surface immediately following formic acid exposure at 150 K (Fig. 1), while further exposure leads to the adsorption of molecular formic acid (Fig. 1). Molecular formic acid desorbs from Pd(1 1 1) on heating to 200 K (Fig. 2) in agreement with previous TPD results where molecular formic acid desorption is found in this temperature range [55] leaving a surface covered by only formate species. Formate species are also formed directly by exposing a Pd(1 1 1) surface heated to 200 K to formic acid, where no co-adsorbed CO is found (Fig. 2). Heating the surface to above 230 K results in thermal decomposition of the formate species (Fig. 2) again in accord with the TPD spectra of formic acid on Pd(1 1 1) [55]. The only disparity between TPD and RAIRS results is that no CO is found on the surface using RAIRS. CO desorption in TPD may be ascribed to CO adsorbing from the background [56].

A formate-covered Pd(1 1 1) surface was prepared by exposure to 5 L of formic acid at 170 K and heating to 200 K and the LEED *I*/*E* curves collected both for the clean and adsorbate-covered surfaces (Fig. 3). Since the formate species do not form an ordered overlayer, the (1×1) Bragg spots were analyzed using method described previously [41–43] to yield an adsorption geometry in which the oxygen atoms of the formate are located approximately above palladium atoms with the OCO plane oriented perpendicular to the surface in accord with the infrared data and the results of previous measurements of formate species on copper [38,39]. The resulting structural parameters are displayed in Table 3 and the geometry depicted in Fig. 5. LEED analyses also indicate that there is no CO co-adsorbed with the formate species (Fig. 6) consistent with infrared results (Figs. 1 and 2).

The relatively high values of the Pendry *R*-factor for the optimum structures are probably related to our approximation of treating the disordered overlayer as one of (1×1) periodicity with scattering factor reduced by Θ. On this approximation, it is not possible to take account of local substrate reconstructions in response to the adsorption. However, unlike the case of an ordered overlayer, the reconstructions around each adsorbate would be expected to be different, as each would be expected to have a different spatial distribution of neighboring adsorbates. Consequently, the best that any diffraction technique could determine might be a *distribution* of different local substrate reconstruction around each adsorbate. As our aim in this work is mainly to determine the configuration of the atoms of the adsorbate relative to the mean substrate, we did not attempt to recover this distribution.

To explore theoretically the possible adsorption geometries of formate on Pd (1 1 1) using DFT, initial configurations were created with the C atom centered above a high-symmetry surface site (atop, bridge, fcc and hcp) and the C–H bond pointed away from the surface along the surface normal. For each such surface site, initial configurations were examined with the C–O bonds oriented along several directions relative to the surface normal and the OCO plane perpendicular to the surface. The C–O bonds were directed in such a manner to ensure that sufficient sites were examined and such that the presumed Pd–O bonds would be close to high symmetry sites. Each configuration was then optimized using energy minimization as previously described. In each case, the initial geometry of the molecule was taken to be that of deprotonated, gas-phase formic acid.

Most of the initial structures moved from their initial high symmetry surface sites to other surface sites during energy minimization. In all calculations, the adsorbed molecule converged to one of two locally stable structures. One stable structure has the C atom centered above an fcc site and the O atoms located above an atop and a bridge site. The second stable structure has the C atom centered above a bridge site and the two O atoms symmetrically located above two atop sites. This second site was calculated to be much more energetically stable than the C-fcc site; the top-bridge-top site is more stable by 0.17 eV/molecule. To ensure that the use of initial configurations with the OCO plane perpendicular to the surface did not affect our final result, we performed several calculations with the top-bridge-top structure with the OCO plane tilted by up to 20° away from the surface normal. In every case, the tilted structures converged to the structure with the un-tilted OCO plane.

In summary, our DFT calculations predict that formate binds on Pd(1 1 1) in a structure with the OCO plane normal to the surface, the C atom centered over a bridge site, and the two O atoms symmetrically located above atop sites. In this structure, the C–O bond lengths are 1.27 Å and these bonds are separated by an angle of 129°. The length of the C–H bond was found to be 1.11 Å and the Pd–O distances were each found to be 2.13 Å. The theoretically determined structural parameters are displayed in Table 3.

5. Conclusions

The structure of ~0.23 monolayers of formate species has been determined on a Pd(1 1 1) surface using low-energy electron diffraction. The molecular plane is oriented perpendicular to the surface with a vector passing through the oxygen atoms being oriented along the short bridge on the (1 1 1) surface. The distance between the oxygen and palladium atoms is 2.16 ± 0.06 Å, the C–O bond length is 1.26 ± 0.05 Å and the OCO bond angle is $130 \pm 5°$. The structure determined by low-energy electron diffraction is in excellent agreement with the results of density functional theory.

Acknowledgment

We gratefully acknowledge support of this work by the U.S. Department of Energy, Division of Chemical Sciences, Office of Basic Energy Sciences, under Grant Nos. DE-FG02-00ER11501 and DE-FG02-03ER15474.

References

[1] D.G. Grenoble, M.M. Estadt, D.F. Ollis, J. Catal. 67 (1981) 90.
[2] A. Kienemann, J.P. Hindermann, R. Brault, H. Idriss, Am. Chem. Soc. Div. Petrol. Chem. 31 (1986) 46.
[3] A. Deluzarche, J.P. Hindemann, R. Kieffer, A. Kienemann, Rev. Chem. Intermed. 6 (1985) 625.
[4] G.C. Chinchen, M.S. Spencer, K.C. Waugh, D.A. Whan, J. Chem. Faraday Trans. I 83 (1987) 333.
[5] G.C. Chinchen, P.J. Denny, D.G. Parker, M.S. Spencer, D.A. Whan, Appl. Catal. 30 (1987) 333.
[6] R. Burch, S. Chalker, J. Pritchard, J. Chem. Soc. Faraday Trans. I 87 (1991) 193.
[7] F. Solymosi, I. Tombácz, M. Kocsis, J. Catal. 75 (1982) 78.
[8] M. Ichikawa and K. Shikakura, in: Proc. 7th Int. Congr. on Catal., Tokyo, Part B, p. 925.
[9] F. Solymosi, A. Erdöhelyi, M. Kocsis, J. Catal. 65 (1980) 428.
[10] F. Solymosi, A. Erdöhelyi, T. Bánsági, J. Catal. 68 (1981) 371.
[11] M.A. Henderson, S.D. Woorley, J. Phys. Chem. 89 (1985) 1417.
[12] T. Izuka, Y. Tanaka, K. Tanabe, J. Mol. Catal. 17 (1982) 381.
[13] Y. Kizukono, S. Kagami, S. Naito, R. Onishi, K. Tamaru, Faraday Disc. Chem. Soc. 72 (1982) 95.
[14] H. Orita, S. Naito, K. Tamaru, J. Catal. 90 (1984) 183.
[15] J.H. Lunsford, Chem. Ind. 22 (1985) 95.
[16] F.L. Moiseev, M.N. Vargaftik, Perspectives in catalysis, in: J.M. Thomas, A. Zhamoriov (Eds.), Chemistry for the 21st Century, Blackwell Science, 1992, p. 91.
[17] B. Samanos, P. Boutry, R. Montarnal, J. Catal. 23 (1971) 19.
[18] C. Egawa, I. Doi, S. Naito, K. Tamaru, Surf. Sci. 176 (1986) 491.
[19] S.W. Jorgensen, R.J. Madix, J. Am. Chem. Soc. 110 (1988) 397.
[20] N.R. Avery, Appl. Surf. Sci. 11/12 (1982) 774.
[21] N.R. Avery, Appl. Surf. Sci. 14 (1982) 149.

[22] R.J. Madix, J.L. Gland, G.E. Mitchell, B.A. Sexton, Surf. Sci. 125 (1982) L574.
[23] J.B. Benziger, G.R. Schoofs, J. Phys. Chem. 88 (1984) 4439.
[24] J.B. Benziger, R.J. Madix, J. Catal. 65 (1980) 49.
[25] N.R. Avery, B.H. Toby, A.B. Anton, W.H. Weinberg, Surf. Sci. 122 (1982) L574.
[26] F. Solymosi, J. Kiss, I. Kovács, Surf. Sci. 192 (1987) 47.
[27] C. Houtman, M.A. Barteau, Surf. Sci. 248 (1991) 57.
[28] M. Bowker, R.J. Madix, Surf. Sci. 102 (1981) 542.
[29] L.H. Dubois, T.H. Ellis, B.B. Zegarski, S.D. Kevan, Surf. Sci. 172 (1986) 385.
[30] M.A. Barteau, M. Bowker, R.J. Madix, Surf. Sci. 94 (1980) 303.
[31] D.A. Outka, R.J. Madix, Surf. Sci. 179 (1987) 361.
[32] B.A. Sexton, R.J. Madix, Surf. Sci. 105 (1981) 177.
[33] N.R. Avery, J. Vac. Sci. Technol. 20 (1982) 592.
[34] R.J. Madix, J.L. Falconer, A.M. Suszko, Surf. Sci. 54 (1976) 6.
[35] G.R. Schoofs, J.B. Benziger, Surf. Sci. 143 (1984) 359.
[36] M. Bowker, R.J. Madix, Appl. Surf. Sci. 8 (1981) 299.
[37] M.A. Barteau, M. Bowker, R.J. Madix, J. Catal. 67 (1981) 118.
[38] D.P. Woodruff, C.F. McConville, A.L.D. Kilcoyne, Th. Linder, J. Somers, M. Surman, G. Paolucci, A.M. Bradshaw, Surf. Sci. 201 (1988) 228.
[39] A. Puschmann, J. Hasse, M.D. Crapper, C.E. Riley, D.P. Woodruff, Phys. Rev. Lett. 54 (1985) 2250.
[40] K.-U. Weiss, R. Dippel, K.-M. Schinlder, P. Gardner, V. Fritsche, A.M. Bradshaw, A.L.D. Kilcoyne, D.P. Woodruff, Phys. Rev. Lett. 69 (1992) 3169.
[41] T. Zheng, W.T. Tysoe, H.C. Poon, D.K. Saldin, Surf. Sci. 543 (2003) 19.
[42] H.C. Poon, M. Weinert, D.K. Saldin, D. Stacchiola, T. Zheng, W.T. Tysoe, Phys. Rev. B. 69 (2004) 035401.
[43] T. Zheng, D. Stacchiola, H.C. Poon, D.K. Saldin, W.T. Tysoe, Surf. Sci. 564 (2004) 71.
[44] D. Stacchiola, L. Burkholder, T. Zheng, M. Weinert and W.T. Tysoe, J. Phys. Chem. B, in press.
[45] NIH Image is available from http://rsb.info.nih.gov/nih-image/.
[46] M. Kaltchev, A.W. Thompson, W.T. Tysoe, Surf. Sci. 391 (1997) 145.
[47] M.A. Van Hove, R. Lin, G.A. Somorjai, Phys. Rev. Lett. 51 (1983) 778.
[48] D.K. Saldin, J.B. Pendry, M.A. Van Hove, G.A. Somorjai, Phys. Rev. B 31 (1985) 1216.
[49] N. Bickel, K. Heinz, Surf. Sci. 163 (1985) 435.
[50] J.B. Pendry, J. Phys. C 13 (1980) 937.
[51] G. Kresse, H. Hafner, Phys. Rev. B 47 (1993) 558.
[52] F. Starrost, E.A. Carter, Surf. Sci. 500 (2002) 323.
[53] P.J. Feibelman, B. Hammer, J.K. Nørskov, F. Wagner, M. Scheffler, R. Stumpf, R. Watwe, J. Dumesic, J. Phys. Chem. B 105 (2001) 4018.
[54] D.R. Lide, E.H.I.R. Frederikse (Eds.), CRC Handbook of Chemistry and Physics, 83rd ed., CRC Press, New York, 2002.
[55] J.L. Davis, M.A. Barteau, Surf. Sci. 256 (1991) 50.
[56] E. Hansen, M. Neurock, J. Phys. Chem. B 105 (2001) 9218.
[57] A. Barbieri and M.A. Van Hove, Symmetrized Automated Tensor LEED package available from M.A. Van Hove.